Applied Catalysis B: Environmental 307 (2022) 120990

Contents lists available at ScienceDirect

Applied Catalysis B: Environmental

journal homepage: www.elsevier.com/locate/apcatb

Dual function materials ($Ru+Na_2O/Al_2O_3$) for direct air capture of CO_2 and in situ catalytic methanation: The impact of realistic ambient conditions

Chae Jeong-Potter [a], Monica Abdallah [a], Cory Sanderson [b], Mark Goldman [a], Raghubir Gupta [b], Robert Farrauto [a,*]

[a] Columbia University, Department of Earth and Environmental Engineering, New York 10027, USA
[b] Susteon Inc., NC 27513, USA

ARTICLE INFO

Keywords:
Dual function material
Direct air capture
CO_2 methanation
Ruthenium catalyst
Alkaline sorbent
Impact of humidity

ABSTRACT

A dual function material (DFM) comprised of 1% Ru, 10% $Na_2O/\gamma - Al_2O_3$ was studied for combined direct air capture (DAC) of CO_2 and catalytic methanation in a temperature swing operation. In the newly proposed operation, the DFM captures CO_2 (400 ppm) from air at ambient conditions. The material is then heated in H_2 to a temperature sufficient for catalytic conversion of the captured CO_2 to renewable natural gas. In this study, we demonstrate high CO_2 adsorption capacity and rates at ambient conditions (25 °C); the adsorbed CO_2 is then successfully catalytically methanated upon heating in H_2. Adsorption was also carried out in humid conditions, more closely simulating ambient air. Adsorption and methane production were greatly improved with stable initial performance. The rate of adsorption is shown to be flowrate-dependent, which is critical for future reactor design.

1. Introduction

As the world endures environmental crises associated with climate change, it is becoming more widely accepted by the scientific community that anthropogenic CO_2 emissions and atmospheric CO_2 concentrations need to be reduced [1–4]. To this end, dual function materials (DFMs) were introduced by Duyar et al. for point-source CO_2 capture and in situ catalytic conversion to methane [5]. DFMs eliminate the need for the energy intensive regeneration of liquid amine solutions and transportation of CO_2. Comprised of both a capture and catalytic component co-dispersed on the same high surface area carrier, the DFM is able to capture CO_2 from incoming flue gas and convert it to a useful product with the introduction of reactive gas (most commonly H_2) [6,7]. The operation of these capture/conversion cycles have thus far been envisioned to be isothermal, operating at around 320 °C by harnessing the sensible heat of typical power plant flue gases [5,8–10].

More recently, the combination of direct air capture of CO_2 (DAC) from ambient sources and subsequent methanation have been of interest. Recognizing that point-source technologies will not curb all CO_2 emissions as efficiencies can never reach 100% and some sectors cannot be decarbonized [11–13], DAC technologies are projected to play a key role in curbing the increasing levels of CO_2 in the atmosphere [14–17]. DFM for DAC has the additional advantage of geographic freedom and, thus, it can be placed aptly near a H_2 source to reduce logistical issues regarding H_2 transportation and storage.

The combination of DAC with subsequent methanation (DACM) was first introduced by Veselovskaya et al. [18]. The authors proposed adsorbing CO_2 at room temperature with a bed of K_2CO_3/Al_2O_3; upon heating to 300–350 °C in the presence of H_2, the CO_2 is desorbed and methanated over a bed of Ru/Al_2O_3 encased in the same reactor [18]. More recently, these authors have shown the use of two separate reactors for adsorption/desorption and subsequent methanation to improve the conversion of CO_2 to CH_4 [19,20]. Subsequently, the DFM (single bed of sorbent and catalyst) has shown that it can be applied for DACM. Our earlier work proved that, like in power plant scenarios, the DFM ($Ru, Na_2O/Al_2O_3$) can capture and methanate CO_2 from simulated ambient air in isothermal operation [21]. Other work has shown that $Ni\text{-}Na/Al_2O_3$ DFM can also be used for DACM in both isothermal and temperature swing operation [22].

We recognize that heating the incoming air to methanation temperatures can be quite energy intensive. Given the low concentrations of CO_2, very large amounts of air must be processed to reach reasonable daily CO_2 removal values (e.g., multiple ton_{CO2}/day). Instead, removing the CO_2 at ambient conditions provides a more economically attractive

* Corresponding author.
E-mail address: rf2182@columbia.edu (R. Farrauto).

https://doi.org/10.1016/j.apcatb.2021.120990
Received 26 September 2021; Received in revised form 15 November 2021; Accepted 30 November 2021
Available online 2 December 2021

technology. We now propose the use of DFM for DACM in a temperature swing operation but still in a single reactor. The use of a single reactor (rather than two separate reactors) can greatly reduce the energy requirement of the process as only a single bed will need to be heated. This will also allow for more continuous operation as multiple reactors can be utilized in parallel. A conceptual schematic of the new process is shown in Fig. 1.

Upon introduction of filtered CO_2 in ambient air, the DFM selectively adsorbs the CO_2, producing CO_2-lean air. Our previous in-situ DRIFTS studies show that for Ru- and Na_2O-containing DFMs, the CO_2 is captured as surface bicarbonate and bidentate carbonate species [23, 24]. Our DRIFTS studies have also shown that the oxygen in air will oxidize the Ru to a catalytically inactive oxide species (i.e., RuO_x or RuO_2 species) [25–27]. Once the sorbent material is saturated, the bed will be heated and H_2 introduced. The RuO_x will have to be reduced to catalytically active Ru, upon which the CO_2 will migrate from the sorbent (Na_2O) to Ru sites to be methanated at a higher temperature. The product stream of methane and water (CH_4 + 2 H_2O) can be treated (e.g., dried and pressurized) to be re-introduced to the existing natural gas infrastructure. To ensure that this process can achieve net-zero emissions, our scale up plan is to engineer the system to provide heat only to the DFM washcoat on the walls of a monolith, using heat generated from renewable sources of energy. Some feasible examples include renewable electricity from solar and wind, concentrated solar, and renewable H_2 powered fuel cells.

Herein, we investigate the efficacy of DFM (Ru+Na_2O/Al_2O_3) for direct air capture of CO_2 at ambient temperature and subsequent catalytic methanation at elevated temperature. We discuss the effect of temperature on adsorption capacity and establish flowrate-dependent rates of adsorption to assist in reactor design and sizing. We then examine the ability of this material to produce methane upon heating. Cyclic performance of the material is also established through some extended cyclic studies in both dry adsorption and humid adsorption conditions. Lastly, a comparative study is performed with a Ru+CaO/Al_2O_3 DFM. The work presented is a material study in which DFMs are evaluated for activity and stability. The DFM is evaluated for activity and stability with the goal of depositing it as an active washcoat on a monolith structure to minimize pressure drop, as is common for the catalytic converter in vehicles.

2. Experimental

2.1. Materials preparation

2.1.1. Ru+Na_2O/Al_2O_3 dual function material

A dual function material (DFM) with 1% Ru catalyst loading and 10% Na_2O adsorbent loading by weight was prepared on 300 μm γ-Al_2O_3 granules (Sasol TH100) using the incipient wetness method. First, an aqueous solution of Na_2CO_3 precursor salt (Sigma Aldrich, >99%) is impregnated (incipient wetness) onto the alumina granules to reach an adsorbent loading of 10% Na_2O. Multiple impregnation steps were needed to reach the target sorbent loading due to the limits of precursor salt solubility. The partially loaded sample was dried overnight (>12 h) in static air at 100 °C between incipient wetness impregnations. A slight excess of solution, with respect to the total pore volume of the granules, was used to favor the uniformity of the DFM batch. Once the target loading was achieved, the sample was calcined for 3 h at 400 °C to decompose the precursor salt and achieve the final sorbent form.

Subsequently, 1% Ru catalyst was impregnated onto the calcined sample using an aqueous solution of ruthenium (III) nitrosyl nitrate (Ru(NO)$(NO_3)_3$) precursor salt (Alfa Aesar, Ru 32%). Again, a slight excess of solution, with respect to total pore volume of the granules, was used during impregnation to favor uniform impregnation of Ru. The Ru-loaded sample was dried for 2 h in static air at 120 °C and subsequently calcined for 3 h at 250 °C to decompose the precursor salt. The final active form of the DFM sample is 1% Ru, 10% "Na_2O"/Al_2O_3 and is denoted as Ru+Na_2O/Al_2O_3 DFM hereafter. This form of the sample is achieved after H_2 pre-treatment before TGA and packed bed experimentation during which methane production is detected, indicating the decomposition of Na_2CO_3 precursor and any chemisorbed CO_2 to "Na_2O". We have seen that realistically there are multiple species of Na present on the DFM surface, thus the designation "Na_2O" [8,10,24]. H_2 pre-treatment conditions are detailed in the following sections.

2.1.2. Ru+CaO/Al_2O_3 dual function material

1% Ru, 10% CaO/Al_2O_3 DFM (denoted Ru+CaO/Al_2O_3 DFM hereafter) was prepared using the methods described in Section 2.1.1. The CaO sorbent was impregnated using an aqueous solution of Ca$(NO_3)_2$•4 H_2O (Sigma Aldrich, 99%), dried, and calcined. Ru was impregnated onto the sorbent-loaded sample using the same procedure described in Section 2.1.1.

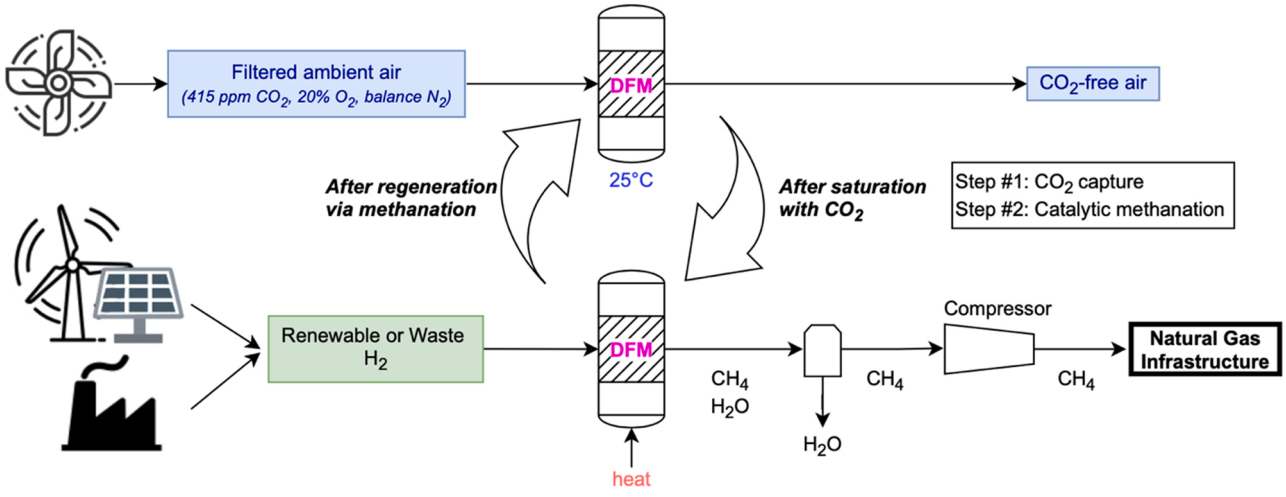

Fig. 1. : Schematic of DACM using DFM in a temperature swing operation.

2.2. Packed bed reactor tests

2.2.1. Reactor set up

All packed bed reactor studies were conducted by loading DFM (on γ-Al_2O_3 granules) in a quartz tube reactor (O.D. = 12.75 mm, I.D. = 10.5 mm, L = 500 mm) and secured with glass wool (Supelco Inc, USA). The remaining space in the reactor was packed with 3 mm diameter glass beads (McKesson, USA) to decrease dead volume. The reactor tube was fitted in a microthermal furnace (MTSC12.5 R x 18–1Z, Mellen, USA) and a K-type thermocouple (Omega, USA) at the middle of the DFM bed for temperature feedback control. Mass flowmeters were used to feed and mix compressed gases at designated flowrates. A saturator at ambient temperature and pressure was placed after the flowmeters to introduce moisture to the system during adsorption. The saturator was bypassed during dry adsorption cycles.

An ice bath was placed at the exit of the reactor to condense any moisture present in the system. Dry exit gas compositions were analyzed at NTP using a LI-830 CO_2 gas analyzer (LI-COR, USA) for ppm-level detection of CO_2 ($\pm$ 2 ppm accuracy) and an Enerac 700 (Enerac, USA) for ppm-level detection of methane and percentages of CO and O_2. A set up of the reactor is shown in Fig. 2.

2.2.2. Adsorption/methanation cycles

Samples of 0.5 g of DFM granules were loaded in a packed bed configuration and pre-treated at 300 °C (heating rate: 5 °C/min) for 3 h with 20% H_2/N_2 at a total flowrate of 16.7 ml/min (GHSV: 2 L(NTP) h^{-1} g_{DFM}^{-1}, 1160 h^{-1}) to ensure complete reduction of RuO_x to catalytically active Ru^0 and to hydrogenate any precursor carbonates.

The following steps were taken for subsequent adsorption/methanation cycles:

1. CO_2 capture step at 25 °C with simulated ambient air (400 ppm CO_2/air) at 400 ml/min (NTP) until saturation (>2 h for dry conditions; >4 h for humid conditions)
2. 15-min purge with N_2 at 100 ml/min (NTP)
3. Heating to 300 °C in 30 min (9–10 °C/min) in 15% H_2/N_2 at 100 ml/min (NTP)
4. Hold at 300 °C for 2 h in 15% H_2/N_2 at 100 ml/min (NTP).

Humid adsorption and methanation cycles were also performed, during which simulated ambient air (400 ppm CO_2/air) was passed through a water saturator at ambient temperature to achieve ~2% H_2O content in the adsorption feed (equivalent to ~90% humidity at 25 °C). The subsequent conditions for heating and 300 °C temperature hold was identical to that described above.

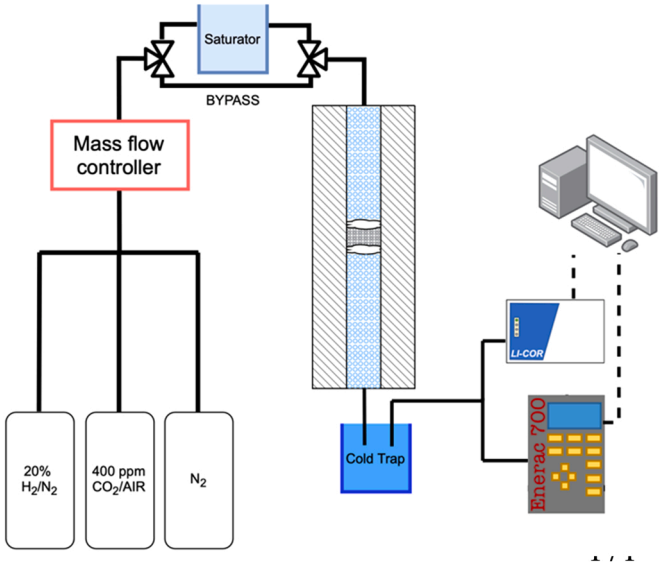

Fig. 2. : Packed bed reactor set up.

2.2.3. Adsorption flowrate test

A 0.5 g sample of Ru+Na_2O/Al_2O_3 DFM granules was loaded into the reactor in a packed bed configuration and pre-treated at 300 °C (heating rate: 5 °C/min) for 3 h with 20% H_2/N_2 at a total flowrate of 16.7 ml/min (GHSV: 2 L(NTP) h^{-1} g_{DFM}^{-1}, 1160 h^{-1}) to the clean surface and ensure the complete reduction of RuO_x to catalytically active Ru^0 as well as hydrogenation of any remaining Na_2CO_3 to "Na_2O." Subsequently, adsorption behavior of Ru+Na_2O/Al_2O_3 DFM was tested by exposing the sample to an adsorption feed of 400 ppm CO_2/air at 25 °C until saturation (i.e. CO_2 concentration at outlet reads ~400 ppm). Four flowrates were tested: 100, 200, 300, and 400 ml/min (NTP). Between each adsorption test, the sample was heated to 300 °C in 30 min in 15% H_2/N_2 (100 ml/min). The sample was held at 300 °C for 4 h in 15% H_2/N_2 to clear the DFM of adsorbed CO_2 by conversion to CH_4.

2.3. Thermal gravimetric analysis (TGA)

All thermal gravimetric studies were performed in a NETZSCH TG 209 F1 Libra unit. For all studies, 30 mg of sample was loaded onto an alumina crucible and dried in the TG unit in N_2 at 120 °C for 3 h. Following drying, samples were pre-reduced in 15% H_2/N_2 at 300 °C for 6 h. All steps were carried out with a total gas flow of 80 ml/min (NTP: normal temperature and pressure; 20 °C and 1 atm) at 1 atm. All heating steps were carried out at 5 K/min and all cooling steps at 10 K/min unless otherwise specified.

2.3.1. Adsorption capacity of Ru+Na_2O DFM at 25 °C and 320 °C

CO_2 adsorption capacity of Ru+Na_2O/Al_2O_3 DFM was studied at two different temperatures. After pre-reduction as described above, the temperature was increased to 320 °C and the sample was exposed to a stream of 375 ppm CO_2, 19% O_2, and balance N_2 for 6 h. After a 30-minute purge with N_2 to evacuate O_2 from the instrument chamber, 15% H_2/N_2 (at 320 °C) was introduced for 6 h to reduce the sample and clear the surface of adsorbed CO_2. The sample was then cooled to 25 °C in N_2 and subsequently exposed to the same adsorption stream (375 ppm CO_2, 19% O_2, and balance N_2) for 6 h. This generated isotherms at 320 and 25 °C.

2.3.2. Temperature programmed reduction (TPR)

Reduction of RuO_x species was tested on Ru+Na_2O/Al_2O_3 DFM (1% Ru, 10% Na_2O/Al_2O_3). After pre-reduction the temperature was reduced to 25 °C and the sample was exposed to a stream of 7.5% O_2/N_2 for 6 h. After a 20-minute inert N_2 purge, the sample was heated in a stream of 15% H_2/N_2 at 10 K/min to 300 °C (TPR).

2.4. H_2 chemisorption

H_2 chemisorption tests were performed on fresh and aged samples of the DFM (1% Ru, 10% "Na_2O"/Al_2O_3 granules before and after humid adsorption cycling) using a ChemBET Pulsar TPR/TPD unit (Quantachrome). H_2 adsorbed per gram of DFM was obtained at 100 °C after in situ reduction in 10% H_2/N_2 (30 ml/min, STP) at 320 °C for 24 h. Dispersion was obtained by assuming that stoichiometry for chemisorption is one H atom per Ru site.

3. Results

3.1. Short-term packed bed aging of Ru+Na_2O/Al_2O_3 DFM in temperature swing operation

The viability of 1% Ru, 10% Na_2O/Al_2O_3 (Ru+Na_2O/Al_2O_3 DFM) for combined DAC and methanation in a temperature swing operation was

tested through a short-term packed bed aging study. The results of 10 cycles of adsorption (dry air) and methanation are shown in Fig. 3.

The DFM adsorbs an average of 550 $\mu mol_{CO2}/g_{DFM}$ at 25 °C. The adsorption performance (black dots) is consistent from cycle to cycle without any major signs of deactivation. The amount of methane produced from cycle to cycle (purple bars) after heating and with a hold at 300 °C is also consistent, averaging about 300 $\mu mol_{CH4}/g_{DFM}$. As a result, 54.5% of the total CO_2 adsorbed was converted to CH_4. Selectivity towards CH_4 is 100% in all cycles and no other products (including CO) were detected.

A major contribution to the observed low CH_4 production is the amount of CO_2 that is desorbed (about 35% of the adsorbed quantity) unreacted during heating. This is an artifact of how H_2 is introduced and how the bed is heated. Fig. 4 shows the profiles of CO_2 desorbed (green solid line) and CH_4 produced (purple solid line) during heating from 25 °C to 300 °C in cycle 10.

During heat up, CO_2 is detected at the reactor outlet starting as low as 50 °C and broad peak between 100 °C and 175 °C is exhibited. After 175 °C, the CO_2 output decreases and CH_4 is detected. Duyar et al. observed that methanation over Ru/Al_2O_3 catalyst also began at 175 °C [8], corroborating the results shown here. CH_4 output peaks between 250 °C and 275 °C, indicating that the highest kinetic rate is achieved beyond 250 °C. The catalytic component of the DFM (i.e. Ru) is oxidized during adsorption due to the presence of O_2; subsequently, the material must be heated to a sufficient temperature to allow the RuO_x species to be reduced to catalytically active Ru^0 before methanation can occur. In addition, the kinetics for methanation must be more favorable than desorption, which can also only be achieved at sufficiently high temperature. As such, desorption of unreacted CO_2 is favored until a sufficiently high temperature is achieved for methanation light-off. This theory was verified with a temperature programmed reduction (TPR) of oxidized $Ru+Na_2O/Al_2O_3$ DFM to determine the temperature at which reduction of the RuO_x species begins. The resulting TG mass change profile found in Fig. 5.

It can be seen that the sample starts losing mass at around 150 °C (gray dashed line) and a fast linear rate of mass lose is achieved after 175 °C, signaling active reduction of the RuO_x species to catalytically active Ru^0. This correlates well with the light-off of methanation seen in Fig. 4 indicating that there is sufficient reduction of the RuO_x to then initiate methanation at 175 °C.

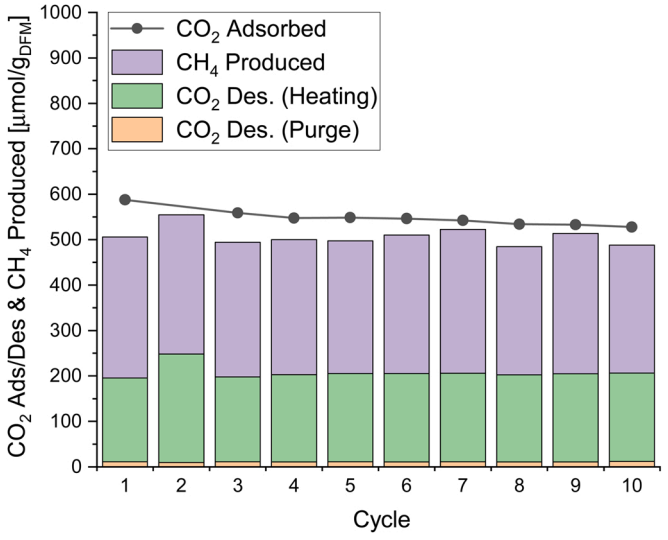

Fig. 3. : CO_2 adsorption (black dots), CO_2 desorption (orange bars and green bars), and CH_4 production (purple bars) for 10 cycles of adsorption/methanation on $Ru+Na_2O$ DFM as follows: i) adsorption at 25 °C in the presence of 400 ppm CO_2/air (dry), ii) heating to 300 °C in 15% H_2/N_2, and iii) 2-hour hold at 300 °C in 15% H_2/N_2. The reactor was purged after adsorption to avoid mixing O_2 and H_2. Experimental details can be found in Section 2.2.2.

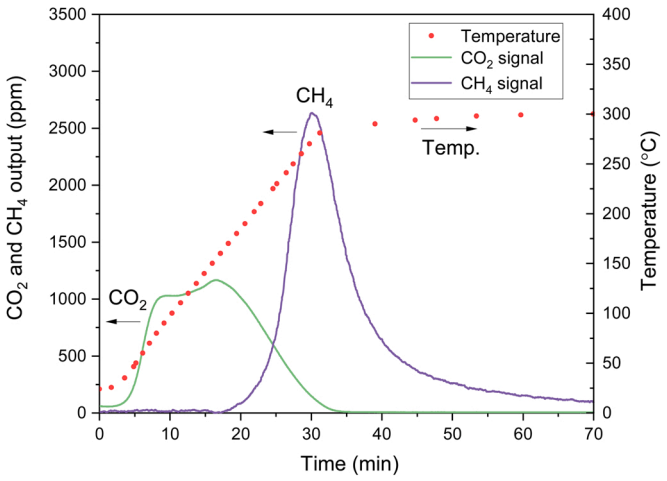

Fig. 4. : CO_2 (green solid line) desorbed and CH_4 (purple solid line) generated with temperature readings (red dots) from 25 °C to 300 °C with 15% H_2/N_2 in packed bed configuration. Profiles correspond to cycle 10 of adsorption/methanation (Fig. 3); experimental conditions can be found in Section 2.2.2.

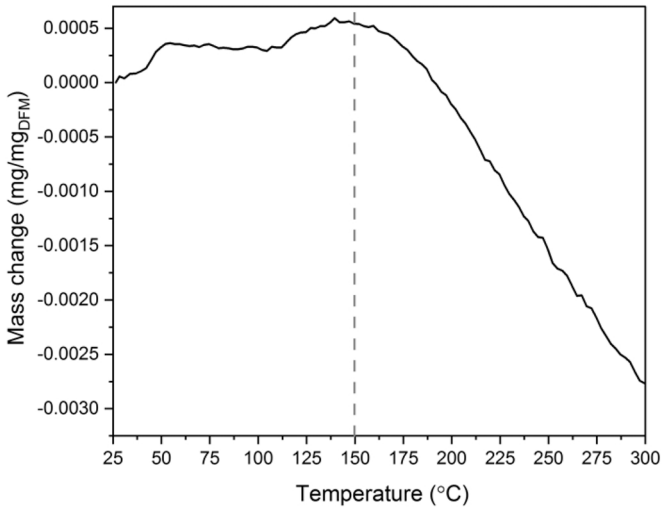

Fig. 5. : TG mass profile for TPR of oxidized $Ru+Na_2O/Al_2O_3$ DFM with 15% H_2/N_2 sweep gas. Temperature at which mass loss is first detected (150 °C) is demarked by a gray dashed line. Experimental conditions can be found in Section 2.3.2.

Identifying techniques to reduce the amount of CO_2 that desorbs during heating will be crucial for increasing CH_4 production (relative to the total CO_2 adsorbed). Strategies for selectively and rapidly heating the washcoat on the monolith will be addressed in future scale up work. In actual application of the DFM, we expect the H_2 source will be in higher concentration (>50% if from waste streams, or better yet pure green H_2 from renewable electrolysis). As a result, it is likely that methane light-off may occur at lower temperatures, thus reducing the amount of CO_2 that is unreacted. It is also possible that the H_2 will be delivered to the system at higher pressure, which would also reduce the methane light-off temperature. In fact, Kosaka et al. have observed positive results by elevating reaction pressures on $Ni-Na/Al_2O_3$. Through their cycles of adsorption (5% CO_2/N_2) and reduction at 450 °C, they showed that methane production increased with reduction pressures (between 0.1 and 0.9 MPa) [22]. Additionally, a TPR of CO_2-loaded $Ni-Na/Al_2O_3$ showed that as pressure increased, the onset methanation temperature decreased [22]. We expect that similar trends

would be observed with our DFM, improving the cyclic conversion of adsorbed CO_2 to CH_4.

3.2. Effect of ambient air humidity (moisture) during adsorption on cyclic performance of $Ru+Na_2O/Al_2O_3$ DFM

Realistic ambient environments for DAC will operate with varying levels of moisture (i.e. humidity). Therefore, it is necessary to test the $Ru+Na_2O/Al_2O_3$ DFM for stable cyclic performance after exposure to humid air during adsorption. Fig. 6 shows the results of 5 cycles of humid adsorption (~2% H_2O, 90% relative humidity at 25 °C) and subsequent methanation. Average results from 10 cycles of dry adsorption and methanation (Fig. 3) are included and labeled "DRY AVG." for comparison to the humid adsorption and methanation cycles (1−5).

Cycles performed with humid air showed overall superior adsorption and methanation with stable performance. In these cycles, the average total CO_2 adsorbed (black dots) was about 1300 $\mu mol_{CO2}/g_{DFM}$, which is a 2.36-fold increase in capture capacity compared to dry cycles. This is most likely due to the formation of $NaHCO_3$ induced by the presence of H_2O [8,28]. Duyar et al. speculated the formation of $NaHCO_3$ on the DFM after exposure to moisture [8] but it has yet to be confirmed. Wang et al. has shown that it is difficult to detect the Na-species that are present on the DFM, particularly by x-ray diffraction, due to their amorphous nature [9].

As a consequence of greater adsorption, average methane production (purple bars) also increased to about 1040 $\mu mol_{CH4}/g_{DFM}$ (3.47 times an average production in dry conditions). Interestingly, the amount of unreacted CO_2 that desorbed during heating (green bars) was only 260 $\mu mol_{CO2}/g_{DFM}$ (~21% compared to 35% for the dry system shown in Fig. 3). This translates to an increase in CH_4 production and an increase in the amount of adsorbed CO_2 that is converted to CH_4 (80% compared to 54.5% for dry adsorption conditions). Once again, we see that product selectivity is 100% towards CH_4. These results show promise in using the $Ru+Na_2O/Al_2O_3$ DFM in a variety of ambient conditions. A series of adsorption temperatures and humidity levels will need to be tested to clearly define the range of adsorption and methanation capacities of this material.

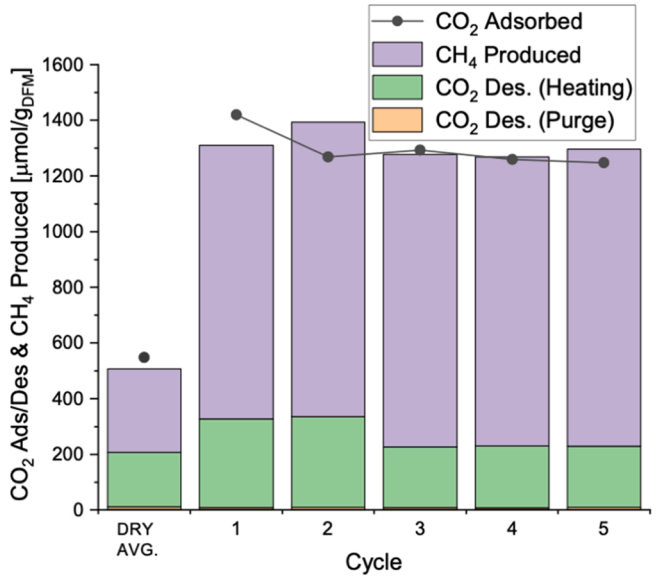

Fig. 6. : CO_2 adsorption (black dots), CO_2 desorption (orange bars and green bars), and CH_4 production (purple bars) for 5 cycles of adsorption/methanation on $Ru+Na_2O/Al_2O_3$ DFM as follows: i) adsorption at 25 °C in the presence of 400 ppm CO_2, ~2% H_2O/air (~90% humidity), ii) heating to 300 °C in 15% H_2/N_2, and iii) 2-hour hold at 300 °C in 15% H_2/N_2. Average results from 10 cycles of dry adsorption and methanation (labeled "DRY AVG.") are shown. Experimental details can be found in Section 2.2.2.

The stability of the $Ru+Na_2O$ DFM after cycling was verified with stable methanation performance and no changes in dispersion as measured by H_2 chemisorption. As seen in Table 1, the cycled material ($Ru+Na_2O$ DFM after 5 cycles of humid adsorption and methanation) maintains similar H_2 adsorption and Ru dispersion values as the fresh material. This indicates that the Ru sites are stable after exposure to high levels of O_2 and moisture during the adsorption followed by methanation up to 300 °C. This is consistent with characterization of our DFMs by TEM and EDS mapping after long term aging in simulated flue gas conditions [9].

3.3. Comparison of $Ru+Na_2O/Al_2O_3$ DFM and $Ru+CaO/Al_2O_3$ DFM: importance of simulating realistic humidity testing conditions

CaO is an alternative sorbent previously investigated in DFMs [5,8,29]; however, Na_2O (in concert with Ru) has been shown to have more favorable kinetics to methanation [30]. Arellano-Treviño et al. reported that CaO-containing DFM required a much longer time for complete methanation of the adsorbed CO_2 and attributed this to the presence of strong carbonates [30]. The presence of strongly bound carbonates is favorable for temperature swing operation where retention of adsorbed CO_2 during heat up needs to be maximized. This is supported by comparing the CO_2 and CH_4 reactor output profiles as a function of temperature as found in Fig. 7.

When comparing the CO_2 desorption profiles of Ru+CaO (solid line) and $Ru+Na_2O$ (dashed line) DFM in Fig. 7a, we see that the initial rate of CO_2 desorption (occurring until about 50 °C) is higher with Ru+CaO. However, the rate of CO_2 desorption from the $Ru+Na_2O$ DFM quickly surpasses this rate; as discussed in Section 3.1, the CO_2 desorption is maintained in peak values between 75 and 175 °C. These values are much higher than the second, broader peak seen on the desorption profile of the Ru+CaO DFM, which spans between 100 °C and 175 °C before tailing off. In general, the Ru+CaO DFM desorption profile is less broad and intense than that of the $Ru+Na_2O$ DFM, equating to less CO_2 desorption upon heating. In the shown cycles, the amount of CO_2 desorbed was 96 $\mu mol_{CO2}/g_{DFM}$ for the Ru+CaO DFM and 195 $\mu mol_{CO2}/g_{DFM}$ for the $Ru+Na_2O$ DFM, indeed showing that Ru+CaO loses less CO_2 during heat up.

In Fig. 7b, we also see that the Ru+CaO DFM (solid line) methane light-off occurs at ~150 °C while for $Ru+Na_2O$ DFM (dashed line) light-off is about 175 °C. Peak CH_4 production with the Ru+CaO DFM at around 260 °C, but at around 270 °C with the $Ru+Na_2O$ DFM. Overall, Ru+CaO DFM shows a higher methane production at 350 $\mu mol_{CH4}/g_{DFM}$ (compared to 280 $\mu mol_{CH4}/g_{DFM}$ with the $Ru+Na_2O$ DFM) due to higher CO_2 retention as exhibited by less desorption. These results were all in the dry adsorption conditions; it is important to determine the effects of humidity on the Ru+CaO DFM. The results of cycling the Ru+CaO for adsorption and methanation in dry and humid adsorption conditions are found in Fig. 8.

As shown in cycles 1–3, cyclic performance of the Ru+CaO DFM in dry adsorption conditions are promising. Though total CO_2 adsorption (averaging 470 $\mu mol_{CO2}/g_{DFM}$) is lower than that of the $Ru+Na_2O$ DFM, methane production averages 360 $\mu mol_{CH4}/g_{DFM}$ (purple bars) with less CO_2 desorbed during heating (green bars, averaging 96 $\mu mol_{CO2}/g_{DFM}$).

Table 1
H_2 chemisorption and Ru dispersion on fresh and cycled $Ru+Na_2O$ DFM (1% Ru, 10% Na_2O/Al_2O_3). The "cycled" material was tested for 5 cycles of humid adsorption at ambient conditions and methanation to 300°C (Fig. 6). Experimental conditions of chemisorption can be found in Section 2.4.

Sample Condition	H_2 adsorbed [μL/g]	Dispersion
Fresh	48.16	4.34%
Cycled	50.72	4.57%

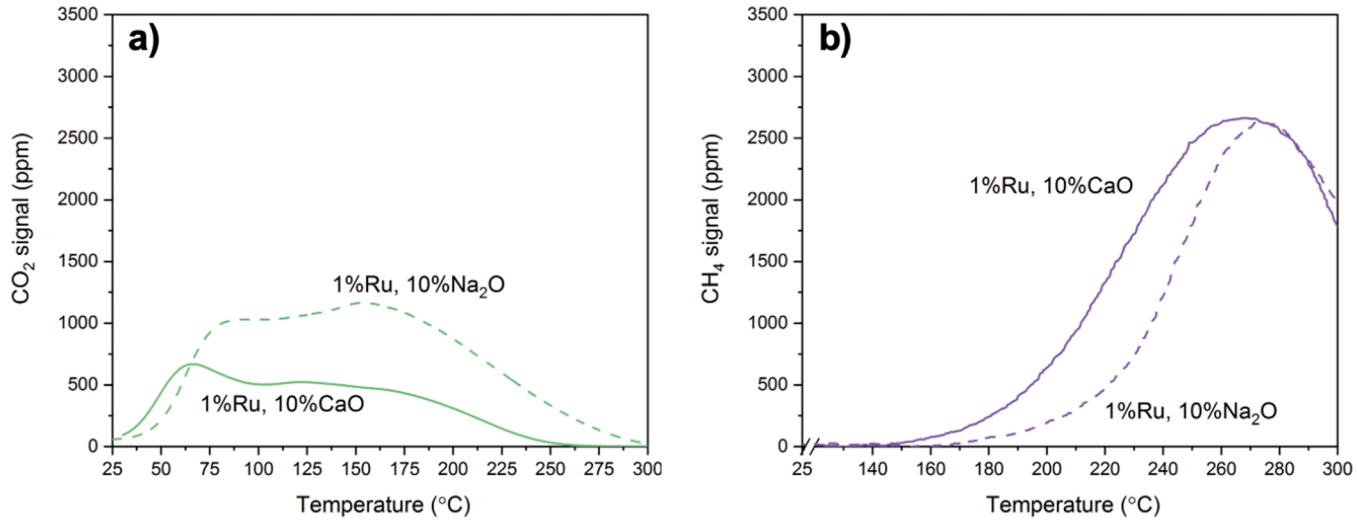

Fig. 7. : Output profiles of (a) CO_2 (green) and (b) CH_4 (purple) as a function of temperature during heating from 25 °C to 300 °C with 15% H_2/N_2 in packed bed configuration. Profiles for Ru+Na_2O/Al_2O_3 DFM (dashed curves) correspond to cycle 10 of dry adsorption/methanation and profiles for Ru+CaO/Al_2O_3 DFM (solid curves) correspond to cycle 3 of dry adsorption/methanation; experimental conditions can be found in Section 2.2.2.

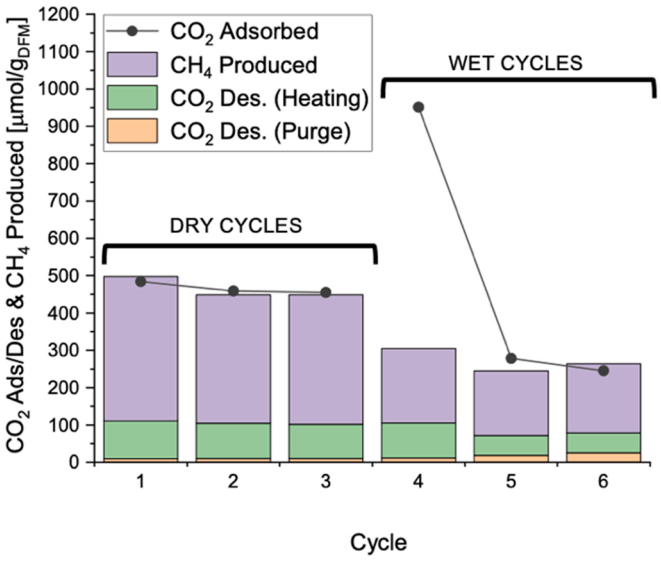

Fig. 8. : CO_2 adsorption (gray dots), CO_2 desorption (orange bars and green bars), and CH_4 production (purple bars) for 6 total cycles of adsorption/methanation on Ru+CaO/Al_2O_3 DFM. Cycles 1–3 (labeled "Dry Cycles") were done with dry adsorption gas (400 ppm CO_2/air) and cycles 4–6 (labeled "Wet Cycles") were done with humid adsorption gas (400 ppm CO_2, ~2% H_2O/air). The cycle steps are as follows: i) adsorption at 25 °C, ii) heating to 300 °C in 15% H_2/N_2, and iii) 2-hour hold at 300 °C in 15% H_2/N_2. Experimental details can be found in Section 2.2.2.

The methane production from CO_2 adsorbed is about 77%.

Significant reduction in methane production is observed in humid adsorption conditions (cycles 4–6). In cycle 4, the total CO_2 adsorption is greatly increased to about 950 $\mu mol_{CO2}/g_{DFM}$, following the same trend seen with the Ru+Na_2O DFM; however, only a small fraction of this CO_2 is either desorbed or methanated (32%), greatly reducing the CO_2 adsorption capacity in the subsequent cycles. In cycles 5 and 6, the adsorption capacity averages to about 260 $\mu mol_{CO2}/g_{DFM}$ and methane production averages to about 180 $\mu mol_{CO2}/g_{DFM}$. This indicates that the Ru+CaO DFM is not a suitable replacement for the Ru+Na_2O DFM under these conditions when attempting to mitigate the desorption of unreacted CO_2.

3.4. *Optimization of the rate of adsorption on Ru+Na_2O/Al_2O_3 DFM for reactor design*

Optimizing the rate of adsorption is critical for reactor sizing and design. First, the effect of temperature was studied through thermal gravimetric analysis (TGA). Adsorption profiles generated at 25 °C and 320 °C are shown in Fig. 9. The high temperature (320 °C) was chosen to represent an isothermal operation case (much like our earlier work in power plant DFM [5,8–10,30] and DAC-DFM [21]). In isothermal operation, 320 °C is preferred for the fastest methanation kinetics and is conveniently in the temperature range of power plant exhausts [9].

The initial rates of adsorption are about the same (1.4×10^{-4} mg_{CO2} mg_{DFM}^{-1} sec^{-1}), suggesting a mass tranfer effect. Clearly, adsorption is favored at 25 °C (blue) compared to 320 °C (red solid line). This is aligned with the fact that CO_2 adsorption onto the DFM is an exothermic process [30]; it is expected that chemical adsorption would be

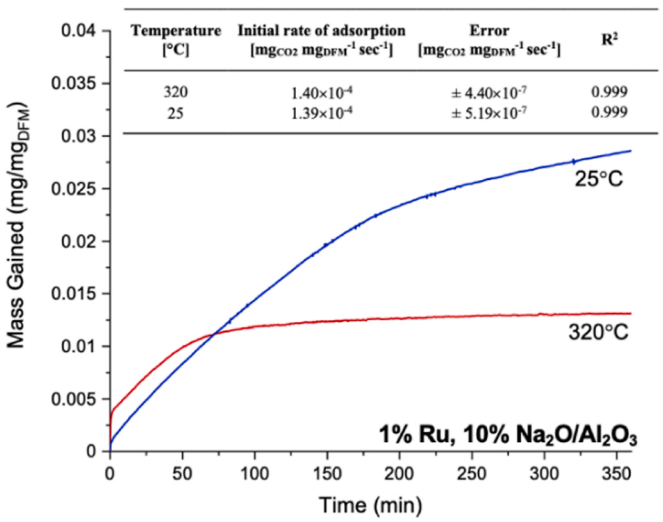

Fig. 9. : TG mass gain profiles of Ru+Na_2O/Al_2O_3 DFM upon exposure to 375 ppm CO_2, 19% O_2, and balance N_2 at 320 °C (red solid line) and 25 °C (blue solid line). Initial rates of CO_2 adsorption as determined by linear fit of mass change profiles between 0.005 and 0.0075 mg/mg_{DFM} of mass gain can be found in embedded table. Experimental conditions can be found in Section 2.3.1.

thermodynamically favored at lower temperatures, hence the greater mass gain observed at 25 °C. Fig. 9 also shows that the rate of adsorption at 25 °C remains in the fast, linear region until well over 100 min of CO_2/air exposure. This indicates that we can maintain fast kinetics while achieving high adsorption capacities.

Four flowrates were tested in a packed bed configuration (Fig. 10) to observe the effect on adsorption behavior. The cumulative amount of CO_2 adsorbed over 2 h shows higher flowrates indeed result in higher initial rates of adsorption. This further confirms that the rate of adsorption in this system is limited by mass transfer of CO_2 (in both transfer through the bulk air and in supply of CO_2 into the system as induced by the low CO_2 concentration). The observed rates of adsorption were quantified by the slopes of the cumulative CO_2 adsorption curves in Fig. 10 as determined by linear fits. These values can be found in Table 2.

As seen in Table 2, a four-fold increase in flowrate results in a 3.88-fold increase in rate (0.229 μmol g_{DFM}^{-1} sec^{-1} with an increase to 400 ml/min). This trend is critical when considering the trade-offs between rate, pressure drop, and power requirements. As flowrate is increased, pressure drop will increase, which will in turn increase power requirements of the fans driving air into the system. In future embodiments of the process, DFM – the active material – will be washcoated onto monoliths in order to reduce pressure drop. The monolith will also reduce energy requirements for heating as just the thin washcoat will need to be heated. Such artifacts have made the monolith a primary choice for applications such as the automotive catalytic converter, which requires low pressure drop and rapid heating.

4. Conclusion

The Ru+Na_2O/Al_2O_3 DFM (1% Ru, 10% Na_2O/Al_2O_3) has been investigated for combined DAC at ambient conditions and subsequent methanation in a temperature swing operation. We have confirmed that this DFM shows reliable cyclic performance for direct air capture (DAC) of 400 ppm CO_2, displaying stable CO_2 adsorption and methane production in a 10-cycle study of dry adsorption/methanation. DFM performance is significantly improved when ambient air is humidified, representative of realistic DAC. Adsorption in humid conditions is 2.36 times greater than in dry conditions, likely as a result of amorphous $NaHCO_3$ formation. Methane production is about 3.5 times greater due to greater retention of the adsorbed CO_2 during heating in H_2. CO_2 desorption is an artifact of our lab-scale studies and can be improved by increasing H_2 partial pressure and/or reaction pressure during heating and methanation. In all cases, selectivity towards CH_4 remained at 100%.

We also identified that adsorption of these low levels of CO_2 is mass transfer limited and can be improved with higher flowrates. However, this will induce pressure drop and, thus, is an important element to consider when designing the reactor and the structure of the DFM configuration. To this point, high open frontal area monolithic substrates are being considered. Still, many other process parameters such as varying ambient conditions for capture of CO_2 reflecting different seasons, times of day, and locations must be tested in order to finalize the reactor design and mode of operation.

Ru+CaO/Al_2O_3 DFM was also explored as an alternative to address the issue of CO_2 desorption during heating. While this material did indeed show that less CO_2 desorbed unreacted it performed poorly in the presence of moisture during the adsorption step. This showed that it is critical to test materials by closely simulating realistic conditions. Ru+Na_2O/Al_2O_3 DFM, therefore, shows the greatest potential for DAC-methanation applications. Further evaluation of this material should include exposure to a variety of ambient environments (i.e. temperature and humidity) as well as long-term cyclic aging studies.

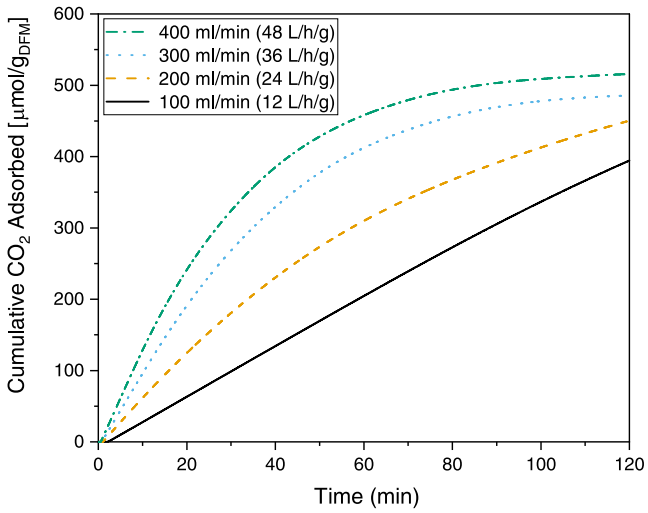

Fig. 10. : Cumulative CO_2 adsorbed over time on Ru+Na_2O DFM at four different flowrates of 400 ppm CO_2/air: 100 ml/min (black solid line), 200 ml/min (yellow dashed line), 300 ml/min (blue dotted line), and 400 ml/min (green dash-dot line). Experimental details for these packed bed tests can be found in Section 2.2.3.

Table 2
Initial rates of CO_2 adsorption on Ru+Na_2O DFM as determined by linear fit of cumulative CO_2 adsorption curves found in Fig. 10. The regression was fit for the first 10 min of the CO_2 adsorption curves. Space velocity is expressed as flowrate per gram of DFM.

Flowrate [ml/min]	Space Velocity [L (NTP) h^{-1} g_{DFM}^{-1}]	Initial rate of adsorption [μmol g_{DFM}^{-1} sec^{-1}]	Error [μmol g_{DFM}^{-1} sec^{-1}]	R^2
100	12	0.059	$\pm 2.93 \times 10^{-7}$	1
200	24	0.108	$\pm 5.36 \times 10^{-5}$	0.999
300	36	0.173	$\pm 2.06 \times 10^{-5}$	1
400	48	0.229	$\pm 3.92 \times 10^{-5}$	1

CRediT authorship contribution statement

Chae Jeong-Potter: Conceptualization, Methodology, Validation, Investigation, Writing – original draft, Visualization, Formal analysis, Supervision. **Monica Abdallah:** Methodology, Validation, Investigation, Writing – review & editing. **Cory Sanderson:** Conceptualization, Validation. **Mark Goldman:** Investigation. **Raghubir Gupta:** Conceptualization, Supervision, Funding acquisition. **Robert J. Farrauto:** Validation, Resources, Writing – review & editing, Supervision, Project administration, Funding acquisition.

Declaration of Competing Interest

The authors declare that they have no known competing financial interests or personal relationships that could have appeared to influence the work reported in this paper.

Acknowledgments

The authors would like to thank the Cohn Memorial Fellowship, the United States Department of Energy (Grant # DE-SC0020795) and Anglo American, UK for their financial support. Our gratitude extends to SASOL, Germany for providing a variety of Al_2O_3 samples for testing.

References

[1] International Energy Agency, Global Energy & CO_2 Status Report, 2019. ⟨https://www.iea.org/geco/emissions/⟩ (accessed 9 May 2019).

[2] IEA, Global Energy Review 2019, 2020. ⟨https://www.iea.org/reports/global-energy-review-2019⟩ (accessed 5 June 2020).

[3] J. Blunden, D.S. Arndt (Eds.), State of the Climate in 2018, 100, Bulletin of the American Meterological Society, 2019.

[4] IPCC, CH02: Mitigation pathways compatible with 1.5°C in the context of sustainable development, in: Special Report: Global Warming of 1.5°C, 2018.

[5] M.S. Duyar, M.A. Arellano, R.J. Farrauto, Dual function materials for CO_2 capture and conversion using renewable H_2, Appl. Catal. B: Environ. 168 (2015) 370–376, https://doi.org/10.1016/j.apcatb.2014.12.025.

[6] P. Melo Bravo, D.P. Debecker, Combining CO_2 capture and catalytic conversion to methane, Waste Dispos. Sustain. Energy 1 (2019) 53–65, https://doi.org/10.1007/s42768-019-00004-0.

[7] I.S. Omodolor, H.O. Otor, J.A. Andonegui, B.J. Allen, A.C. Alba-Rubio, Dual-Function Materials for CO_2 Capture and Conversion: A Review, Ind. Eng. Chem. Res. 59 (2020) 17612–17631, https://doi.org/10.1021/acs.iecr.0c02218.

[8] M.S. Duyar, S. Wang, M.A. Arellano-treviño, R.J. Farrauto, CO_2 utilization with a novel dual function material (DFM) for capture and catalytic conversion to synthetic natural gas: An update, J. CO2 Util. 15 (2016) 65–71, https://doi.org/10.1016/j.jcou.2016.05.003.

[9] S. Wang, R.J. Farrauto, S. Karp, J.H. Jeon, E.T. Schrunk, Parametric, cyclic aging and characterization studies for CO_2 capture from flue gas and catalytic conversion to synthetic natural gas using a dual functional material (DFM), J. CO2 Util. 27 (2018) 390–397, https://doi.org/10.1016/j.jcou.2018.08.012.

[10] M.A. Arellano-treviño, N. Kanani, C.W. Jeong-potter, R.J. Farrauto, Bimetallic catalysts for CO_2 capture and hydrogenation at simulated fl ue gas conditions, Chem. Eng. J. 375 (2019), 121953, https://doi.org/10.1016/j.cej.2019.121953.

[11] M. Ge, K. Lebling, K. Levin, J. Friedrich, Tracking Progress of the 2020 Climate Turning Point, Washington, DC, 2019.

[12] D. Leeson, N. Mac Dowell, N. Shah, C. Petit, P.S. Fennell, A. Techno-economic, analysis and systematic review of carbon capture and storage (CCS) applied to the iron and steel, cement, oil refining and pulp and paper industries, as well as other high purity sources, Int. J. Greenh. Gas. Control 61 (2017) 71–84, https://doi.org/10.1016/j.ijggc.2017.03.020.

[13] M. Fasihi, O. Efimova, C. Breyer, Techno-economic assessment of CO_2 direct air capture plants, J. Clean. Prod. 224 (2019) 957–980, https://doi.org/10.1016/j.jclepro.2019.03.086.

[14] K. Lackner, H.-J. Ziock, P. Grimes, Carbon capture from air, is it an option?, in: 24th Annual Technical Conference on Coal Utilization & Fuel Systems, Clearwater, FL, 1999.

[15] D. Keith, M. Ha-duong, J. Stolaroff, Climate strategy with CO_2 capture from the air, Clim. Change 74 (2006) 17–45.

[16] D.W. Keith, Why capture CO_2 from the atmosphere? Science 325 (2009) 1654–1655, https://doi.org/10.1126/science.1175680.

[17] C.W. Jones, CO_2 Capture from Dilute Gases as a Component of Modern Global Carbon Management, Annu. Rev. Chem. Biomol. Eng. 2 (2011) 31–52, https://doi.org/10.1146/annurev-chembioeng-061010-114252.

[18] J.V. Veselovskaya, P.D. Parunin, O.V. Netskina, A.G. Okunev, A Novel Process for Renewable Methane Production: Combining Direct Air Capture by K_2CO_3 / Alumina Sorbent with CO_2 Methanation over Ru / Alumina Catalyst, in: Topics in Catalysis, 61, 2018, pp. 1528–1536, https://doi.org/10.1007/s11244-018-0997-z.

[19] J. v Veselovskaya, P.D. Parunin, O. v Netskina, L.S. Kibis, A.I. Lysikov, A. G. Okunev, Catalytic methanation of carbon dioxide captured from ambient air, Energy 159 (2018) 766–773, https://doi.org/10.1016/j.energy.2018.06.180.

[20] J. v Veselovskaya, A.I. Lysikov, O. v Netskina, D. v Kuleshov, A.G. Okunev, K_2CO_3-containing composite sorbents based on thermally modified alumina: synthesis, properties, and potential application in a direct air capture/methanation process, Ind. Eng. Chem. Res. 59 (2020) 7130–7139, https://doi.org/10.1021/acs.iecr.9b05457.

[21] C. Jeong-Potter, R. Farrauto, Feasibility Study of Combining Direct Air Capture of CO_2 and Methanation at Isothermal Conditions with Dual Function Materials, Appl. Catal. B: Environ. 282 (2021), 119416, https://doi.org/10.1016/j.apcatb.2020.119416.

[22] F. Kosaka, Y. Liu, S.Y. Chen, T. Mochizuki, H. Takagi, A. Urakawa, K. Kuramoto, Enhanced activity of integrated CO_2 capture and reduction to CH4 under pressurized conditions toward atmospheric CO_2 utilization, ACS Sustain. Chem. Eng. 9 (2021) 3452–3463, https://doi.org/10.1021/acssuschemeng.0c07162.

[23] C.J. Keturakis, F. Ni, M. Spicer, M.G. Beaver, H.S. Caram, I.E. Wachs, Monitoring solid oxide CO_2 capture sorbents in action, ChemSusChem 7 (2014) 3459–3466, https://doi.org/10.1002/cssc.201402474.

[24] L. Proaño, E. Tello, M.A. Arellano-Trevino, S. Wang, M. Cobo, R.J. Farrauto, In-situ DRIFTS study of two-step CO_2 capture and catalytic methanation over Ru,"Na_2O"/Al_2O_3 Dual Functional Material, Appl. Surf. Sci. 479 (2019) 25–30, https://doi.org/10.1016/j.apsusc.2019.01.281.

[25] F. Garisto, Thermodynamic Behaviour of Ruthenium At High Temperatures, AECL-9552, Whiteshell Nuclear Research Establishment, 1988.

[26] E. Guglielminotti, F. Boccuzzi, M. Manzoli, F. Pinna, M. Scarpa, Ru/ZrO_2 Catalysts: I. O_2, CO, and NO Adsorption and Reactivity, J. Catal. 192 (2000) 149–157, https://doi.org/10.1006/jcat.2000.2835.

[27] L. Proaño, M.A. Arellano-Treviño, R.J. Farrauto, M. Figueredo, C. Jeong-Potter, M. Cobo, Mechanistic assessment of dual function materials, composed of Ru-Ni, Na_2O/Al_2O_3 and Pt-Ni, Na_2O/Al_2O_3, for CO_2 capture and methanation by in-situ DRIFTS, Appl. Surf. Sci. 533 (2020), 147469, https://doi.org/10.1016/j.apsusc.2020.147469.

[28] A. Samanta, A. Zhao, G.K.H. Shimizu, P. Sarkar, R. Gupta, Post-combustion CO_2 capture using solid sorbents: A review, Ind. Eng. Chem. Res. 51 (2012) 1438–1463, https://doi.org/10.1021/ie200686q.

[29] C. Janke, M.S. Duyar, M. Hoskins, R. Farrauto, Catalytic and adsorption studies for the hydrogenation of CO_2 to methane, Appl. Catal. B: Environ. 152– 153 (2014) 184–191, https://doi.org/10.1016/j.apcatb.2014.01.016.

[30] M.A. Arellano-Treviño, Z. He, M.C. Libby, R.J. Farrauto, Catalysts and adsorbents for CO_2 capture and conversion with dual function materials: Limitations of Ni-containing DFMs for flue gas applications, J. CO2 Util. 31 (2019) 143–151, https://doi.org/10.1016/j.jcou.2019.03.009.